Journal of Electrical Engineering & Technology (2020) 15:1177–1187
https://doi.org/10.1007/s42835-020-00398-6

ORIGINAL ARTICLE

A Review of State-of-the-art Techniques for PMSM Parameter Identification

Hanwoong Ahn[2] · Hyunjong Park[3] · Changhyun Kim[4] · Hyungwoo Lee[1]

Received: 25 July 2019 / Revised: 22 October 2019 / Accepted: 26 February 2020 / Published online: 9 March 2020

Abstract
In this paper, a review of previous research in d- and q-axis inductance identification techniques for permanent magnet synchronous motor (PMSM) is presented. The d- and q-axis inductances have an important influence on both the transient and steady-state responses of PMSM. Therefore, their accurate information is essential not only for predicting the responses but also for designing system controllers. However, standardized procedures for the PMSM inductance identification have not yet been established. The main purpose of this paper is to provide an understanding of the various parameter identification methods. Conventional techniques are reviewed and introduced with their inherent advantages and drawbacks.

Keywords PMSM drives · Inductance identification · Offline identification · Online identification

1 Introduction

Recently, permanent magnet synchronous motors are widely used in industrial applications for high efficiency and high output density. As shown in Fig. 1, there are mainly three kinds of synchronous motors. PMSM drivers generally have closed-loop control systems, based on vector control method. Vector control is one of the most popular controls for PMSM, known as decoupling or field orientated control (FOC). It decouples three phase stator currents into two phase d- and q-axis currents which produce the flux and torque, respectively such that it allows direct control of flux and torque.

Therefore, the exact information of the d- and q-axis inductances is indispensable for successful controller design. If the exact inductances of PMSM cannot be measured or estimated, it may occur as a result of low-efficient operation, output power reduction and even out-of-synchronization. In addition, PMSM has a severe local self-saturation and cross-saturation effects, so PMSM parameters such as resistance and d- and q-axis inductances are changed nonlinearly by conditions such as electric current, phase angle, etc. In particular, the d- and q-axis inductances change irregularly depending on the mechanical power, shape, and operating characteristics of motor, so the incorrect estimation of parameters cause the performance degradation of the control systems. Thus, accurate estimation of the inductances that change in real-time is a necessary element for designing the controller and ensuring the improved control performance.

The estimation methods are categorized into two methods: the offline and online parameter estimations according to the estimation time in system operation.

The offline parameter estimation techniques are classified according to the implementation point at standstill or operating conditions. The estimation techniques at the standstill conditions include the DC current decay test and AC standstill methods. On the other hand, the estimation techniques for the operating conditions include the vector-controlled method and generator test. The offline parameter estimation

✉ Hyungwoo Lee
krhwlee@ut.ac.kr

Hanwoong Ahn
ahnhw@kari.re.kr

Hyunjong Park
hyuntou@kari.re.kr

Changhyun Kim
chkim@jvision.ac.kr

1 Department of Railway Vehicle System Engineering, Korea National University of Transportation, Chungju, Korea

2 Satellite Bus Development Division, Korea Aerospace Research Institute, Daejeon, Korea

3 Launcher Control System Team, Korea Aerospace Research Institute, Daejeon, Korea

4 Department of Electricity, VISION College of Jeonju, Jeonju, Korea

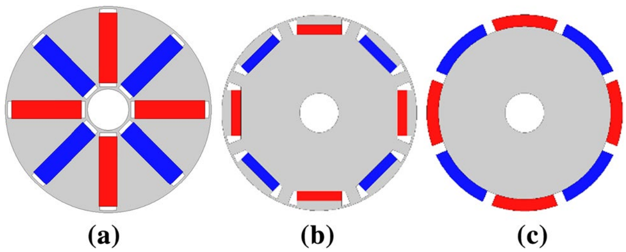

Fig. 1 Classification according to rotor shape of PMSM. **a** Spoke-type permeant magnet synchronous motor. **b** Interior buried permanent magnet synchronous motor. **c** Surface mounted permanent magnet synchronous motor

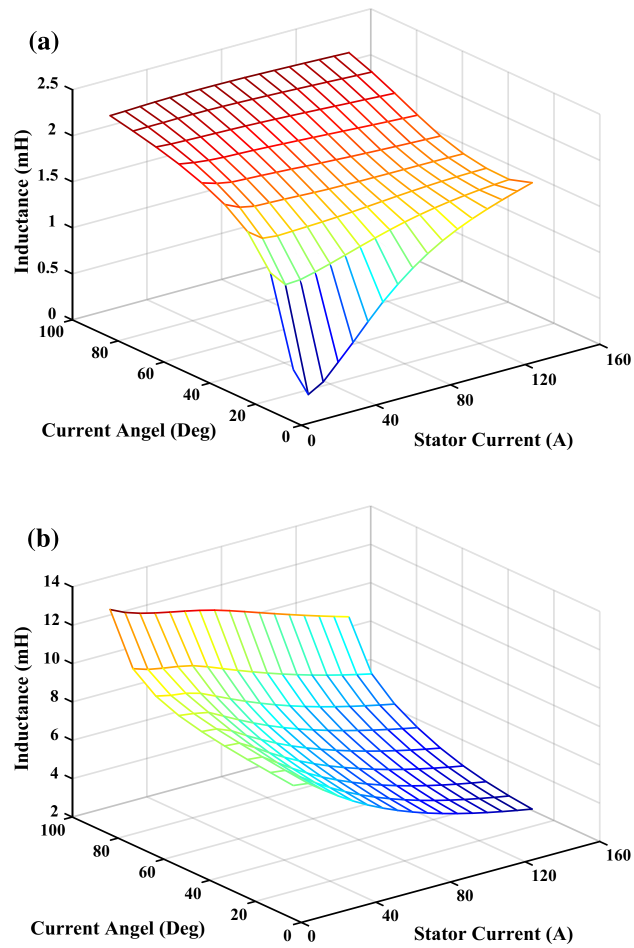

Fig. 2 d- and q-axis Inductances following Stator Current and Current Phase Angle. **a** d-axis inductance **b** q-axis inductance

methods have the merit to be easily understood by its simple algorithm. However, there still exist disadvantages to require additional equipment and measurement error caused by the estimation at the single operating point.

Meanwhile, the online parameter estimation techniques include the model reference adaptive control techniques, recursive least square based techniques, extended Kalman filter based techniques, and artificial neural network techniques. The online parameter estimation techniques are appropriate for applications with various operation ranges, because they are performed during the system operation. However, the high-efficient microprocessor is required for dealing with the relatively complex procedure. In this paper, the state-of-the-art offline and online parameter identification techniques are entirely reviewed and summarized by researching the conventional and recent advancement of parameter identification methods for PMSM.

2 IPMSM Equivalent Circuit

For vector control of IPMSM, the three-phase voltage equation of IPMSM is converted into the d-q axes voltage equation as in (1) through Clarke transformation and Park transformation.

$$\begin{bmatrix} v_{ds}^r \\ v_{qs}^r \end{bmatrix} = \begin{bmatrix} R_a & -\omega L_q \\ \omega L_d & R_a \end{bmatrix} \begin{bmatrix} i_{ds}^r \\ i_{qs}^r \end{bmatrix} + \begin{bmatrix} 0 \\ \omega_e \Psi_a \end{bmatrix} \tag{1}$$

where

p: differential operator.
R_a: stator resistance.
ψ_a: permanent magnet flux linkage.
L_d, L_q: d-axis and q-axis stator inductance.
v_{ds}, v_{qs}: d-axis and q-axis stator voltages in rotor frame.
i_{ds}, i_{qs}: d-axis and q-axis stator currents in rotor frame.
ω_e: electrical stator angular velocity.

The stator resistance is easily measured through DC test [1–6], and permanent magnetic flux linkage is obtained by the residual flux density of permanent magnet. However, as shown in Fig. 2, L_d and L_q are nonlinearly changed according to the d- and q-axis current, and their cross-coupling effect [7–9]. Therefore, a technique for accurately estimating L_d and L_q is certainly required for designing various control algorithms such as predicting torque and flux-weakening capabilities. Various estimation methods to obtain the exact values of L_d and L_q have been increasingly studied. That is the reason why this paper focuses on analyzing and classifying these techniques in order to provide a complete guideline.

3 Offline Parameter Estimation Techniques

3.1 DC Current Decay Test

In the DC current decay test maintains the rotor on the d-axis or q-axis of the stator in order to measure the inductance of the u-phase DC current which decreases

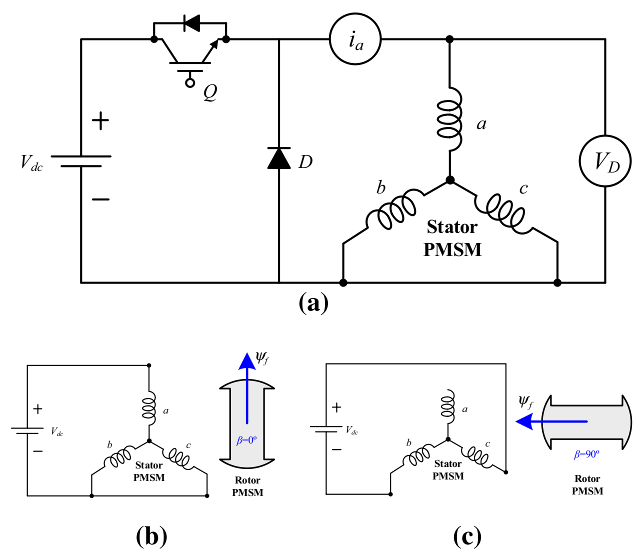

Fig. 3 **a** Connection diagram for measuring the L_d, L_q. **b** Connecting to align the direct axis. **c** Connecting to align the quadrature axis

from rated current to zero [10–25]. The test configuration is depicted in Fig. 3a. The test consists of the two stages to apply a step voltage onto the stator winding of the machine at a standstill and to measure the corresponding voltage and current. The procedures to fix the rotor in d- and q-axis direction by applying stator voltage are illustrated in Fig. The inductances are obtained by

$$L_d = \frac{\left[\int_0^\infty \frac{2}{3} V_{dD}(t)dt + R_s \int_0^\infty i_{da}(t)dt\right]}{i_{da0}} \tag{2}$$

$$L_q = \frac{\left[\int_0^\infty \frac{2}{3} V_{qD}(t)dt + R_s \int_0^\infty i_{qa}(t)dt\right]}{i_{qa0}} \tag{3}$$

The advantages of DC current decay test are that the test equipment is simple and easy to measure [22]. But, because the test is executed only at the stationary state, it inevitably has inductance errors and iron loss not considered during operating state [26].

In [16] dealing with these drawbacks, the armature of synchronous machine is supplied at standstill by DC-Chopper, pseudo random binary sequences (PRBS) voltages, PWM voltages and DC decay. The methods described in [23] are performed to determine the optimum set of the measured samples in order to gain the machine's parameters. An extended DC decay test technique for arbitrary positions of the rotor is proposed in [24]. Another DC current decay test is described in [14], in which the method is proposed in order to measure it with regard to saturation and cross saturation effects.

3.2 AC Standstill Method

In the ac standstill method for the IPMSM, the currents and voltages of this phase and another phase are measured under the standstill condition to supply the single phase sinusoidal voltage [27–36]. So, d- and q-axis inductances are calculated from the self and mutual inductances of the stator winding. The *a*-phase self and *a* and *c*-phase mutual inductance are expressed as a function of the electrical angle

$$L = L_{ls} + L_0 - L_1 \cos 2\theta_r \tag{4}$$

$$M = -M_0 - M_1 \cos 2\left(\theta_r - \frac{\pi}{3}\right) \tag{5}$$

where L_{ls} is leakage inductance, L_0, M_0 are dc term of the self and mutual inductances, L_1, M_1 represent second-harmonic components of the self and mutual inductances. The self and mutual inductances of the others can be expressed in the same way.

The d- and q-axis inductances are obtained by using Park's transformation as follows:

$$L_d = L_{ls} + \left(L_0 - M_0\right) - \left(L_1/2 + M_1\right) \tag{6}$$

$$L_q = L_{ls} + \left(L_0 - M_0\right) + \left(L_1/2 + M_1\right) \tag{7}$$

The connection diagram for testing is reported in Fig. 4. One of the phase windings is excited by AC supply such that the line current and induced phase voltages in one of the other two windings are measured at different rotor positions. At each rotor position, the self and mutual inductances are calculated by Eqs. (8) and (9).

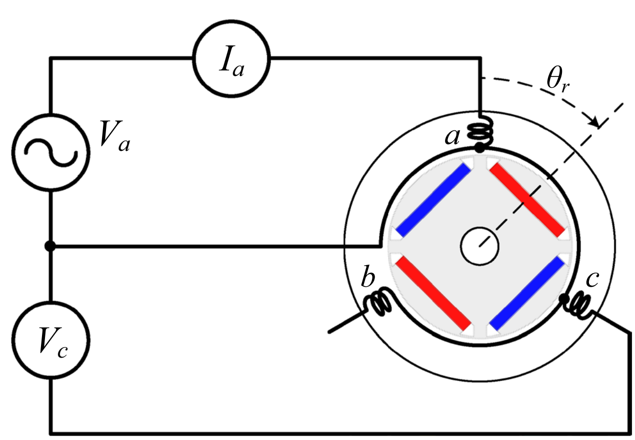

Fig. 4 Circuit connection of the ac standstill test

$$L_a = \frac{\sqrt{\left(V_a/I_a\right)^2 - R_s^2}}{2\pi f} \tag{8}$$

$$M_{ac} = \frac{V_c}{2\pi f I_a} \tag{9}$$

The parameters L_{ls}, L_0, M_0, L_1 and M_1 are determined by (8) and (9) such that d- and q-axis inductances are calculated by (6) and (7).

Even though the AC standstill test gives the simplicity and relatively better accuracy on the estimation of the inductances, it still has the problem of not reflecting the actual operating conditions because the inductance of IPMSM was measured only in the condition of standstill. Also, there exists the time-consuming factor because of the high number of measurements and long measurement times.

In [34], the multi-sine AC standstill test is introduced for the swift identification, by which the effect of saturation, cross saturation, and frequency on the d- and q-axis parameters are rapidly evaluated with a VSI for signal generation. Another improved AC standstill test is described in [27], which the d- and q-axis currents that are produced by the two single phase currents passing through the proposed circuit are identical with that produced by the three phase currents at running condition. In [35], a 3-phase AC voltage source is applied such that the vector control drive is not required. Hence, it is very suitable for normal laboratory experiments since the d- and q-axis inductances are estimated, simultaneously considering the saturation and cross-magnetizing effect. The method in [32] focuses on the new PMSM model with the stator iron loss. Using this model, the d- and q-axis inductances and the equivalent iron loss resistance on the stator are measured by AC standstill test.

3.3 Vector Control Method

The vector control method is based on terminal measurements of the fundamental voltage and current peaks and their phases with respect to the rotor position [33, 37–42]. The a-phase current, voltage, and rotor position are measured by a current probe, a differential probe, and a position sensor, respectively.

Shown in Fig. 5, the d- and q-axis current are calculated from the a-phase current waveform and the rotor position. Similarly, from the measured amplitude and the phase of the fundamental of the voltage, the d- and q-axis voltages are obtained.

The d- and q-axis flux linkages can be calculated by

$$v_d = i_d R_s - \omega_e \phi_q \tag{10}$$

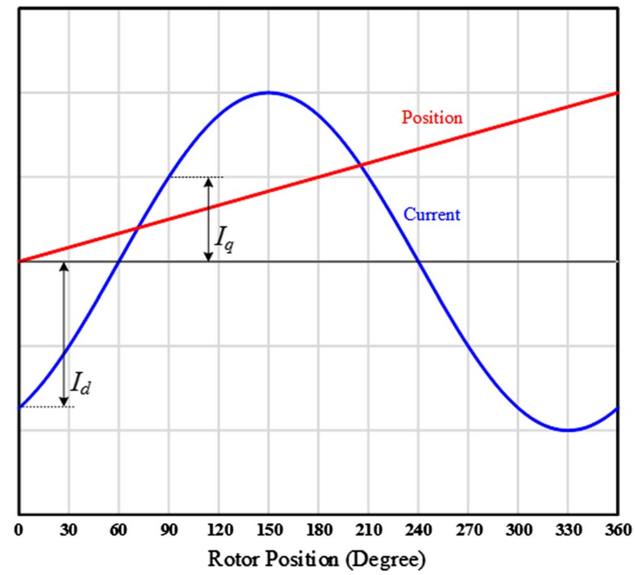

Fig. 5 Calculation of the individual d and q components from the measured current and the phase relationship [37]

$$v_q = i_q R_s + \omega_e \phi_d \tag{11}$$

If the magnet flux is constant and the cross-coupling inductances are zero, the d- and q-axis inductance can be directly estimated from the flux linkages.

The d- and q-axis inductance as follows

$$L_d\left(i_d,\ i_q\right) = \frac{\phi_d - \phi_f}{i_d} \tag{12}$$

$$L_q\left(i_d,\ i_q\right) = \frac{\phi_q}{i_q} \tag{13}$$

Since vector control method are based on the measured voltages and currents, estimated parameters include the effect of saturation and cross-coupling effects. Vector control method is also used to estimate the inductance of the motor even with space harmonics. However, the vector controlled method requires the extra equipment such as the dynamometer, the oscilloscope and the position sensor.

3.4 Other Methods

The other existing approaches to off-line inductance estimation are based on finite element method, described in [7, 43–47]. The methods of [43, 46] calculate motor parameters considering magnetic nonlinearity by using equivalent magnetic circuits, whereas the procedures of [44 ,7] consider the saturation and cross-coupling effects.

The method to obtain the parameters of PMSM without torque measurement has been proposed in [48], in which there are advantages with taking into account iron losses, avoiding uncertainties due to the value of copper resistance. In [49], the inductances are identified by injecting high-frequency signal to the estimated d- and q-axes. The method considers the detailed identification error caused by the inverter nonlinearity influence at different rotor positions.

Reference [50] provides the well summarized review on the off-line synchronous inductance estimation methods.

4 Online Parameter Estimation Techniques

4.1 Recursive Least Square

This group of methods uses known parameters, such as voltages and currents, to identify unknown parameters through mathematical models [51–65]. Unknown parameters can be found to minimize the error between observation and estimation.

Mathematical model of least squares is expressed as

$$Y(k) = \Theta^T(k)Z(k) \tag{14}$$

where $Y(k)$ is the output, $\Theta(k)$ is the unknown parameter vector of the model and $Z(k)$ is the input vector.

The unknown parameter vector $\Theta(k)$ can be obtained from the known vectors $Y(k)$ and $Z(k)$ by a general recursive least square method. The unknown parameters of the mathematical model can be obtained by

$$\varepsilon_i(k) = \left(Y(k) - \hat{\Theta}(k)Z(k)\right)^2 \tag{15}$$

where $\varepsilon_i(k)$ is the square value of the prediction error and $\hat{\Theta}(k)$ is the estimated parameter matrix.

By minimizing the least square function from (14), the estimated parameters are determined by the discrete time approach with respect to the parameter matrix $\Theta(k)$, as follows:

$$\hat{\Theta}(k) = \hat{\Theta}(k-1) + K(k)\left(Y(k) - Z^T(k)\hat{\Theta}(k-1)\right) \tag{16}$$

$$K(k) = P(k-1)Z(k)\left(\lambda I + Z^T(k)P(k-1)Z(k)\right)^{-1} \tag{17}$$

$$P(k) = \left(I - K(k)Z^T(k)\right)P(k-1)/\lambda \tag{18}$$

where $K(k)$ is the gain matrix which updates parameters proportional to the error, $P(k)$ is covariance matrix which must be definite and λ is forgetting factor given by $0 < \lambda < 1$. The mathematical model for RLS is obtained from voltage equations of IPMSM. The observation consists of the indirect reference stator voltage and the measured stator current.

Generally, in the RLS method, the influence of the noise on the parameter identification is trivial, as shown in [56]. However, when the four parameters are simultaneously estimated by using the RLS algorithm, it imposes a heavy burden on the controller and could not be converged on the solution due to poorness of available data. Thus, in [60], the method for estimating the d- and q-axis inductances at the sampling rate and estimating the resistance and torque constant in a separate program executed at a lower frequency is proposed. In [54, 57], the model of the estimated rotating reference frame is used for the parameter identification method.

Since the RLS parameter estimator uses the fixed gain, the accuracy of the estimation is not guaranteed without the parameter variation, and the disturbance observer could provide the unstable transient response characteristic. Parameter fluctuation and inaccuracy in real-time estimation lead to degrading system performances.

4.2 Model Reference Adaptive System based Techniques

The model reference adaptive system (MRAS) is the very popular control method tuned by control factors that can be updated according to the change of system responses. The output of the system is compared to the desired response from the reference model, which is independent of d- and q-axis inductances but the adjustable model dependents on these parameters. The error signal is input to the adaptation mechanism. The output of the adaptation mechanism is determined in order to apply to tuning the adjustable model and also for feedback. The d- and q-axis inductances are corrected based on this error [66–78]. The stability of the closed loop estimator is ensured using Popov's hyper-stability theory. Figure 6 shows the structure of the MRAS.

Based on MEAS, the identified algorithm of d- and q-axis inductances can be written as

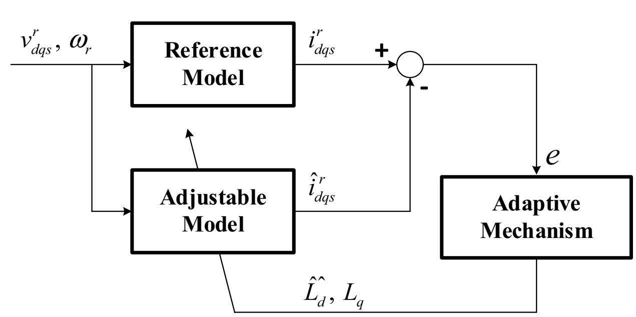

Fig. 6 Structure of MRAS scheme for inductance estimation

$$\hat{L}_d(t) = \hat{L}_d(0) + k_1 \int_0^t \left(i_q - \hat{i}_q\right) d\tau + k_2\left(i_q - \hat{i}_q\right) \tag{19}$$

$$\hat{L}_q(t) = \hat{L}_q(0) + k_1 \int_0^t \left(i_d - \hat{i}_d\right) d\tau + k_2\left(i_d - \hat{i}_d\right) \tag{20}$$

The MRAS method is relatively easy to estimate the motor parameters, so it is applied to solve the voltage imbalance of inverter or converter [73]. Also, the L_d and L_q estimation methods of the motor using this technique can accurately obtain the estimated values under various conditions.

However, the error of the d- and q- axis inductance directly affecting the stator current command has a vital influence on the motor efficiency, so the stator resistance must be estimated to compensate the voltage drop component. This method also has drawbacks in that it is difficult to design the adaptive mechanism and synchronize the PI gain at various operating points.

4.3 Artificial Neural Network (ANN) Techniques

The artificial neural networks have single or multi-layers consisting of input and output, which requires less computation and gives faster convergence time compared to other algorithms such as MRAS and extended Kalman filter (EKF) [79–85]. In [80–83], The adaptive linear neuron (adaline) networks with only inputs and outputs are used to estimate the parameters. The ANN structure for the PMSM is shown in Fig. 7.

The mathematical model of adaline neural networks is as

$$O\left(W_i, X_i\right) = \sum_{i=0}^{n} W_i X_i \tag{21}$$

where X_i is the inputs, W_i is the weights and $O(W_i,X_i)$ is the activation function.

A learning control mechanism samples the inputs, the output, and the desired output and uses these to adjust the weights. The weighting adjustment is obtained through the least mean square (LMS) algorithm as follows:

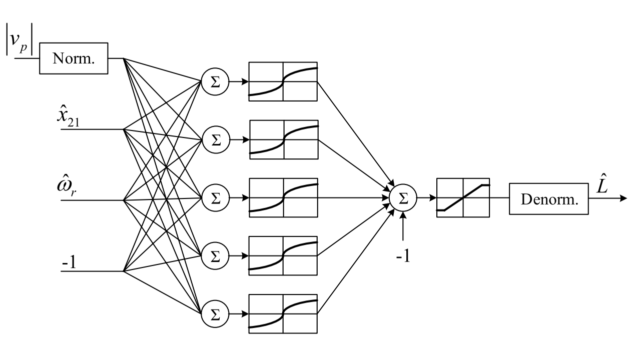

Fig. 7 ANN structure for PMSM

$$W_i(t+1) = W_i(t) + 2\eta\left[d(t) - O\left(W_i, X_i\right)\right] X_i(t) \tag{22}$$

where 0 < i < 1 and η is the learning rate and usually is a small number between 0 and 1 (typically η < 1/n).

In [85], the harmonics in the rotor flux linkage is considered and the corresponding torque ripple is minimized by on-line torque constant estimation. A novel feature of adaptive online weights and biases up-dating of the ANN has also been included in [84]. The method of [79] consists of four layered feed-forward neural networks with an input layer, an output layer and two hidden layers.

Using a neural network, it is possible to calculate parameter variations such as inductance, armature resistance and back emf constant for motor drive in real-time and to enable high performance and robustness control. The controller of the neural network can reduce the computational complexity and simplify the control method, thus constituting a more practical and efficient control system for the IPMSM drive system by vector control. In addition, field weakening control is implemented by using neural network in order to achieve fast response by minimum loss in operating range. However, there is a large inductance error when the initial value is inaccurate.

4.4 Extended Kalman Filter (EKF) Based Techniques

The extended Kalman filter is an optimal recursive estimator for nonlinear systems [70, 75, 86–90]. It provides a solution that considers the effects of the disturbance noises including system and measurement noises. The EKF is developed in the discrete-time state by taking into account the nonlinear model of the IPMSM as follows

$$\begin{cases} x_k = f\left(x_{k-1}, u_{k-1}\right) + w_{k-1} \\ y_k = h\left(x_k\right) + v_k \end{cases} \tag{23}$$

where f is the system transition function, h is the measurement function and u_{k-1} is the control input. w_{k-1} and v_k are process and output noise respectively. They are assumed to be zero mean Gaussian white noises with covariance Q_k and R_k respectively.

For the EKF, mathematically, the predictor step is given by

$$\begin{cases} \hat{x}_{k|k-1} = f\left(\hat{x}_{k-1|k-1}, u_{k-1}\right) \\ P_{k|k-1} = F_{k-1} P_{k-1|k-1} F_{k-1}^T + Q_{k-1} \end{cases} \tag{24}$$

And the corrector step is given by

$$\begin{cases} K_k = P_{k|k-1} H_k^T \left(H_k P_{k|k-1} H_k^T + R\right)^{-1} \\ \hat{x}_{k|k} = \hat{x}_{k|k-1} + K_k\left(y_k - H_k \hat{x}_{k|k-1}\right) \\ P_{k|k} = \left(I - K_k H_k\right) P_{k|k-1} \end{cases} \tag{25}$$

In (23) and (24), P_k is the covariance matrix corresponding to the state estimation error and K_k is called the Kalman

Table 1 Comparison of PMSM Parameter Identification Techniques

	Method	Test equipment	Programming complexity	Computational time	Nonliearity	Accuracy
Offline parameter estimation techniques	DC current decay test	Simplicity	Very low	Very less	Not considered	Less
	AC standstill method	Slightly simplicity	Very low	Less	Slightly considered	Slightly less
	Vector control method	Complexity	Slightly high	High	Considered	Slightly high
Online parameter estimation techniques	Recursive Least Square	Simplicity	High	Slightly high	Considered	Slightly high
	Model Reference Adaptive System	Simplicity	Medium	Medium	Considered	Medium
	Artificial Neural Network	Simplicity	Slightly high	Slightly high	Considered	Medium
	Extended Kalman Filter	Simplicity	Very high	Very high	Considered	High

filter gain. After both the prediction and correction steps have been performed then $\hat{x}_k$ is the current estimate of the states and y_k can be calculated directly from it. Both $\hat{x}_k$ and P_k are stored and used in the predictor step of the next time period. The state transition and observation matrices are defined to be the following Jacobians

$$F_{k-1} = \left.\frac{\partial f}{\partial x}\right|_{\hat{x}_{k-1|k-1},\, u_{k-1}}, \quad H_k = \left.\frac{\partial h}{\partial x}\right|_{\hat{x}_{k|k-1}} \tag{26}$$

The EKF is a recursive optimal filter with the ability to estimate the state variables of a nonlinear system with the minimized estimation error variance so that the state variables and parameters of the system in a noise environment can be estimated appropriately. In addition, the EKF can estimate the parameters from the mathematical model of the device through the process of measurement noise covariance matrices from operating input–output data.

However, the EKF may fail to converge on the appropriate state values if the system model is inaccurate. It also processes input data with noise repeatedly which may lead to a high computational burden.

4.5 Other Methods

As another on-line parameter estimation technique, affine projection algorithm is reported in [91, 92]. The d- and q-axis stator inductances are estimated at high convergence rate, while the stator resistance, the magnetic flux linkage, and the motor torque are estimated at slow convergence rate. Therefore, the estimated parameters and motor torque from the affine projection algorithms can be used to continuously update the control gains for the adaptive controllers.

A direct method of calculating the phase inductance is proposed in [93], which calculates the phase inductance from the phase voltage equations. In [94], the motor parameters are estimated by tuning the controller gains that cancel the pole of the motor transfer function. The real-time estimation algorithms proposed by [95–97] identify the inductance matrix including the rotor position from current harmonics generated by inverter.

5 Conclusion

The inductance is an essential parameter of PMSM to design a controller to obtain high-performances with respect to torque, speed, or sensorless controls. The various research outputs on inductance identification techniques for PMSM are introduced and summarized in this paper.

The inductance estimation techniques of PMSM are classified into off-line and on-line parameter identification methods according to the operating time. The pros and cons of off-line parameter estimation, DC decay, AC standstill, vector controlled and other methods, and on-line parameter identification methods, RLS, MRAC, ANN, EKF and introduced other methods, are analyzed with the viewpoint of the applicability, responding performance, robustness against the disturbance and noise, and calculation complexity. PMSM parameter identification techniques introduced in this paper are summarized in Table 1.

Most of the significant identification methods popular in an industry are categorized into the criteria systems and dealt with in this paper, even if there exist the untouched techniques for lack of space. We attempted to provide the sufficient references for a better understanding of readers with various research backgrounds.

Acknowledgements This work is supported by the Korea Agency for Infrastructure Technology Advancement (KAIA) grant funded by the Ministry of Land, Infrastructure and Transport (Grant 20CTAP-C151867-02).

References

1. Han YS, Choi JS, Kim YS (2000) Sensorless PMSM drive with a sliding mode control based adaptive speed and stator resistance estimator. IEEE Trans Magn 36(5):3588–3591

2. Nahid-Mobarakeh B, Meibody-Tabar F, Sargos FM (2004) Mechanical sensorless control of PMSM with online estimation of stator resistance. IEEE Trans Ind Appl 40(2):457–471
3. Lee K-W, Jung D-H, Ha I-J (2004) An online identification method for both stator resistance and back-EMF coefficient of PMSMs without rotational transducers. IEEE Trans Ind Electron 51(2):507–510
4. Rashed M, MacConnell PFA, Stronach AF, Acarnley P (2007) Sensorless indirect-rotor-field-orientation speed control of a permanent-magnet synchronous motor with stator-resistance estimation. IEEE Trans Ind Electron 54(3):1664–1675
5. Wilson SD, Stewart P, Stewart J (2012) Real-time thermal management of permanent magnet synchronous motors by resistance estimation. IET Electr Power Appl 6(9):716–726
6. Hinkkanen M, Tuovinen T, Harnefors L, Luomi J (2012) A combined position and stator-resistance observer for salient PMSM drives: design and stability analysis. IEEE Trans Power Electron 27(2):601–609
7. Štumberger B, Štumberger G, Dolinar D, Hamler A, Trlep M (2003) Evaluation of saturation and cross-magnetization effects in interior permanent-magnet synchronous motor. IEEE Trans Ind Appl 39(5):1264–1271
8. Rabiei A, Thiringer T, Alatalo M, Grunditz E (2016) Improved maximumtorque-per-ampere algorithm accounting for core saturation, cross-coupling effect and temperature for a PMSM intended for vehicular applications. IEEE Trans Transp Electrif 2(2):150–159
9. Liang W, Fei W, Luk PCK (2016) An improved sideband current harmonic model of interior PMSM drive by considering magnetic saturation and cross-coupling effects. IEEE Trans Ind Electron 63(7):4097–4104
10. Sellschopp FS, Arjona MA (2006) DC decay test for estimating d-axis synchronous machine parameters: a two-transfer-function approach. IEE Proc Electr Power Appl 153(1):123–128
11. Pérez JNH, Hernandez OS, Caporal RM, Magdaleno JDJR, Barreto HP (2013) Parameter identification of a permanent magnet synchronous machine based on current decay test and particle swarm optimization. IEEE Lat Am Trans 11(5):1176–1181
12. Horning S, Keyhani A, Kamwa I (1997) On-line evaluation of a round rotor synchronous machine parameter set estimated from standstill time-domain data. IEEE Trans Energy Convers 12(4):289–296
13. Zhang J, Radun AV (2006) A new method to measure the switched reluctance motor's flux. IEEE Trans Ind Appl 42(5):1171–1176
14. Kilthau A and Pacas JM (2001) Parameter-measurement and control of the synchronous reluctance machine including cross saturation. In proceedings of Conf. Rec. IEEE IAS Annu. Meeting, Chicago, USA, Sep./Oct. 2001.
15. Sellschopp FS, Arjona MA (2005) A tool for extracting synchronous machines parameters from the dc flux decay test. Comput Electr Eng 31(1):56–68
16. Hasni M, Touhami O, Ibtiouen R, Fadel M, Caux S (2008) Synchronous machine parameter identification by various excitation signals. Electr Eng 90(3):219–228
17. Turner PJ, Reece ABJ, Macdonald DC (1989) The D.C. decay test for determining synchronous machine parameters: measurement and simulation. IEEE Trans Energy Convers 4(4):616–623
18. Tumageanian A, Keyhani A (1995) Identification of synchronous machine linear parameters from standstill step voltage input data. IEEE Trans Energy Convers 10(2):232–240
19. Sharma VK, Murthy SS, Singh B (1999) An improved method for the determination of saturation characteristics of switched reluctance motors. IEEE Trans Instrum Meas 48(5):995–1000
20. Kamwa I, Viarouge P, Dickinson EJ (1991) Identification of generalized models of synchronous machine from time-domain tests. IEE Proc C 138(6):485–498
21. Hasni M, Touhami O, Ibtiouen R, Fadel M, Caux S (2010) Estimation of synchronous machine parameters by standstill tests. Math Comput Simul 81(2):277–289
22. Boje ES, Balda JC, Harley RG, Beck RC (1990) Time-domain identification of synchronous machine parameters from simple standstill tests. IEEE Trans Energy Convers 5(1):164–175
23. Groza VZ (2003) Experimental determination of synchronous machine reactances from DC decay at standstill. IEEE Trans Instrum Meas 52(1):158–164
24. Vicol L, Xuan MT, Wetter R, Simond J-J, Viorel IA (2006) On the identification of the synchronous machine parameters using standstill DC decay test. In Proceedings of ICEM 2006 Conference, Chania, Greece.
25. Sandre-hernandez O, Morales-caporal R, Rangel-magdaleno J, Peregrina-barreto H, Hernandez-perez JN (2015) Parameter identification of PMSMs using experimental measurements and a PSO algorithm. IEEE Trans Instrum Meas 64(8):2146–2154
26. Boldea I (1996) Reluctance synchronous machines and drives. Oxford University Press, Oxford
27. Y. Gao, R. Qu, and Y. Liu (2013) An improved AC standstill method for inductance measurement of interior permanent magnet synchronous motors. In Proceedings of 2013 ICEMS, Busan, South Korea.
28. Cavagnino A, Lazzari M, Profumo F, Tenconi A (2000) Axial flux interior PM synchronous motor: parameters identification and steady-state performance measurements. IEEE Trans Ind Appl 36(6):1581–1588
29. Balda JC, Fairbrain RE, Harley RG, Rodgerson JL, Eiteberg E (1987) Measurement of synchronous machine parameters by a modified frequency response method—Part II: Measured results. IEEE Trans. Energy Convers. EC-2(4):646–651
30. Touhami O, Guesbaoui H, Iung C (1994) Synchronous machine parameter identification by a multitime scale technique. IEEE Trans Ind Appl 30(6):1600–1608
31. Dedene N, Pintelon R, Lataire P (2003) Estimation of a global synchronous machine model using a multiple-input multiple-output estimator. IEEE Trans Energy Convers 18(1):11–16
32. Senjyu T, Urasaki N, Simabukuro T, Uezato K (1998) Modelling and parameter measurement of salient-pole permanent magnet synchronous motors including stator iron loss. Math Comput Model Dyn Syst 4(3):219–230
33. Dutta R, Rahman MF (2006) A comparative analysis of two test methods of measuring d - and q -axes inductances of interior permanent-magnet machine. IEEE Trans Magn 42(11):3712–3718
34. Vandoorn TL, De Belie FM, Vyncke TJ, Melkebeek JA, Lataire P (2010) Generation of multisinusoidal test signals for the identification of synchronous-machine parameters by using a voltage-source inverter. IEEE Trans Ind Electron 57(1):430–439
35. Sun T, Kwon SO, Lee JJ, Hong JP (2009) An improved AC standstill method for testing inductances of interior PM synchronous motor considering cross-magnetizing effect. In Proceedings of IEEE Energy Conversion Congress and Exposition (ECCE-2009), San Jose, USA.
36. Chiba A, Nakamura F, Fukao T, Rahman MA (1991) Inductances of cageless reluctance-synchronous machines having nonsinusoidal space distributions. IEEE Trans Ind Appl 27(1):44–51
37. Rahman KM, Hit S (2005) Identification of machine parameters of a synchronous motor. IEEE Trans Ind Appl 41(2):557–565
38. Nee H-P, Lefevre L, Thelin P, Soulard J (2000) Determination of d and q reactances of permanent-magnet synchronous motors without measurements of the rotor position. IEEE Trans Ind Appl 36(5):1330–1335
39. Choi C, Lee W, Kwon SO, Hong JP (2013) Experimental estimation of inductance for interior permanent magnet synchronous machine considering temperature distribution. IEEE Trans Magn 49(6):2990–2996

40. Schaible U, Szabados B (1999) Dynamic motor parameter identification for high speed flux weakening operation of brushless permanent magnet synchronous machines. IEEE Trans Energy Convers 14(3):486–492
41. Štumberger B, Kreča B, Hribernik B (1999) Determination of parameters of synchronous motor with permanent magnets from measurement of load conditions. IEEE Trans Energy Convers 14(4):1413–1416
42. Ertan HB, Şahin I (2012) Evaluation of inductance measurement methods for PM machines. In Proceedings of 2–12 XXth ICEM, Marseille, France.
43. Lee J-Y, Lee S-H, Lee G-H, Hong J-P, Hur J (2006) Determination of parameters considering magnetic nonlinearity in an interior permanent magnet synchronous motor. IEEE Trans Magn 42(4):1303–1306
44. Meessen KJ, Thelin P, Soulard J, Lomonova EA (2008) Inductance calculations of permanent-magnet synchronous machines including flux change and self- and cross-saturations. IEEE Trans Magn 44(10):2324–2331
45. Vaseghi B, Takorabet N, Meibody-Tabar F (2009) Fault analysis and parameter identification of permanent-magnet motors by the finite-element method. IEEE Trans Magn 45(9):3290–3295
46. Kim WH, Kim MJ, Lee KD, Lee JJ, Han JH, Jeong TC, Cho SY, Lee J (2014) Inductance calculation in IPMSM considering magnetic saturation. IEEE Trans Magn 50(1):1–4
47. Chen YS, Zhu ZQ, Howe D (2005) Calculation of d- and q-axis inductances of PM brushless AC machines accounting for skew. IEEE Trans Magn 41(10):3940–3942
48. Fernández-Bernal F, García-Cerrada A, Faure R (2001) Determination of parameters in interior permanent-magnet synchronous motors with iron losses without torque measurement. IEEE Trans Ind Appl 37(5):1265–1272
49. Wang G, Qu L, Zhan H, Xu J, Ding L, Zhang G, Xu D (2014) Self-commissioning of permanent magnet synchronous machine drives at standstill considering inverter nonlinearities. IEEE Trans Power Electron 29(12):6615–6627
50. Gao Y, Qu R, Chen Y, Li J, Xu W (2014) Review of off-line synchronous inductance measurement method for permanent magnet synchronous machines. In Proceedings of ITEC Asia-Pacific, Beijing, China.
51. Tadokoro D, Morimoto S, Inoue Y, and Sanada M (2014) Method for auto-tuning of current and speed controller in IPMSM drive system based on parameter identification. In Proceedings of IPEC-Hiroshima 2014 - ECCE ASIA, Hiroshima, Japan.
52. Morimoto S, Sanada M, Takeda Y (2006) Mechanical sensorless drives of ipmsm with online parameter identification. IEEE Trans Ind Appl 42(5):1241–1248
53. Yoshimi M, Hasegawa M, and Matsui K (2010) Parameter identification for IPMSM position sensorless control based on unknown input observer. In Proceedings of ISIEA, Penang, Malaysia.
54. Ichikawa S, Tomitat M, Doki S, Okuma S (2006) Sensorless control of synchronous reluctance motors based on extended emf models considering magnetic saturation with online parameter identification. IEEE Trans Ind Appl 42(5):1264–1274
55. Inoue Y, Kawaguchi Y, Morimoto S, Sanada M (2011) Performance improvement of sensorless ipmsm drives in a low-speed region using online parameter identification. IEEE Trans Ind Appl 47(2):798–804
56. Inoue Y, Yamada K, Morimoto S, Sanada M (2009) Effectiveness of voltage error compensation and parameter identification for model-based sensorless control of IPMSM. IEEE Trans Ind Appl 45(1):213–221
57. Ichikawa S, Tomita M, Doki S, Okuma S (2006) Sensorless control of permanent-magnet synchronous motors using online parameter identification based on system identification theory. IEEE Trans Ind Electron 53(2):363–372
58. Nguyen QK, Petrich M, and Roth-Stielow J (2014) Implementation of the MTPA and MTPV control with online parameter identification for a high speed IPMSM used as traction drive. In Proceedings of IPEC-Hiroshima 2014 - ECCE ASIA, Hiroshima, Japan.
59. Weijie L, Dongliang L, Qiuxuan W, Lili C, and Xiaodan Z (2016) A novel deadbeat-direct torque and flux control of IPMSM with parameter identification. In Proceedings of EPE'16 ECCE Europe, Karlsruhe, Germany.
60. Underwood SJ, Husain I (2010) Online parameter estimation and adaptive control of permanent-magnet synchronous machines. IEEE Trans Ind Electron 57(7):2435–2443
61. Phowanna P, Boonto S, Konghirun M (2015) Online parameter identification method for IPMSM drive with MTPA. In Proceedings of 2015 18th ICEMS, Pattaya, Thailand.
62. Kim S, Lee H, Kim K, Bae J, Im J, Kim C, Lee J (2009) Torque ripple improvement for interior permanent magnet synchronous motor considering parameters with magnetic saturation. IEEE Trans Magn 45(10):4720–4723
63. Xu Y, Parspour N, Vollmer U (2014) Torque rippleminimization using online estimation of the stator resistances with consideration of magnetic saturation. IEEE Trans Ind Electron 61(9):5105–5114
64. Le LX, Wilson WJ (1988) Synchronous machine parameter identification: a time domain approach. IEEE Trans Energy Convers 3(2):241–248
65. Mouni E, Tnani S, Champenois G (2008) Synchronous generator modelling and parameters estimation using least squares method. Simul Model Pract Theory 16(6):678–689
66. Gatto G, Marongiu I, Serpi A (2013) Discrete-time parameter identification of a surface-mounted permanent magnet synchronous machine. IEEE Trans Ind Electron 60(11):4869–4880
67. Piippo A, Hinkkanen M, Luomi J (2009) Adaptation of motor parameters in sensorless PMSM drives. IEEE Trans Ind Appl 45(1):203–212
68. Boileau T, Leboeuf N, Nahid-Mobarakeh B, Meibody-Tabar F (2011) Online identification of PMSM parameters: parameter identifiability and estimator comparative study. IEEE Trans Ind Appl 47(4):1944–1957
69. An Q, Sun L (2008) On-line parameter identification for vector controlled PMSM drives using adaptive algorithm. In Proceedings of VPPC, Harbin, China.
70. Shi Y, Sun K, Huang L, Li Y (2012) Online identification of permanent magnet flux based on extended kalman filter for IPMSM drive with position sensorless control. IEEE Trans Ind Electron 59(11):4169–4178
71. Hamida MA, De Leon J, Glumineau A, Boisliveau R (2013) An adaptive interconnected observer for sensorless control of pmsynchronous motorswith online parameter identification. IEEE Trans Ind Electron 60(2):739–748
72. Mohamed YARI, Lee TK (2006) Adaptive self-tuning MTPA vector controller for IPMSM drive system. IEEE Trans Energy Convers 21(3):636–644
73. Liu K, Zhu ZQ, Zhang Q, Zhang J (2012) Influence of nonideal voltage measurement on parameter estimation in permanent-magnet synchronous machines. IEEE Trans Ind Electron 59(6):2438–2447
74. Hasegawa M, Matsui K (2009) Position sensorless control for interior permanent magnet synchronous motor using adaptive flux observer with inductance identification. IET Electr Power Appl 3(3):209–217
75. Boileau T, Nahid-Mobarakeh B, Meibody-Tabar F (2008) On-line Identification of PMSM parameters: model-reference vs EKF. In Proceedings of IEEE IAS Annu. Meeting, Edmonton, Canada.
76. Ohnishi K, Matsui N, Hori Y (1994) Estimation, identification, and sensorless control in motion control system. Proc IEEE 82(8):1253–1265

77. Liu L, Cartes DA (2007) Synchronisation based adaptive parameter identification for permanent magnet synchronous motors. IET Control Theory Appl 1(4):1015–1022
78. Keerthi VD, Kumar JSVS (2013) Model reference adaptive control based parameters estimation of permanent magnet synchronous motor drive. Int J Appl or Innov Eng Manag 2(8):267–275
79. Kumar R, Gupta RA, Bansal AK (2007) Identification and control of PMSM using artificial neural network. In Proceedings of 2007 ISIE, Vigo, Spain.
80. Liu K, Zhang Q, Chen J, Zhu ZQ, Zhang J (2011) Online multiparameter estimation of nonsalient-pole PM synchronous machines with temperature variation tracking. IEEE Trans Ind Electron 58(5):1776–1788
81. Liu K, Zhu ZQ (2014) Online estimation of the rotor flux linkage and voltage-source inverter nonlinearity in permanent magnet synchronous machine drives. IEEE Trans Power Electron 29(1):418–427
82. Liu K, Zhu ZQ, Stone DA (2013) Parameter estimation for condition monitoring of PMSM stator winding and rotor permanent magnets. IEEE Trans Ind Electron 60(12):5902–5913
83. Qin H, Liu K, Zhang Q, Shen A, Zhang J (2010) Online estimating voltage source inverter nonlinearity for PMSM by adaline neural network. In Proceedings of 2010 BIC-TA, Changsha, China.
84. Rahman M, Hoque MA (1998) On-line adaptive artificial neural network based vector control of permanent magnet synchronous motors. IEEE Trans Energy Convers 13(4):311–318
85. Liu T, Husain I, Elbuluk M (1998) Torque ripple minimization with on-line parameter estimation using neural networks in permanent magnet synchronous motors. In Proceedings of 1998 IEEE Ind. Appl. Conf., St. Louis, USA.
86. Sim H, Lee J, Lee K (2014) On-line parameter estimation of interior permanent magnet synchronous motor using an extended kalman filter. J Electr Eng Technol 9(2):600–608
87. Song W, Shi SS, Chao C, Gang Y, Qu ZJ (2009) Identification of PMSM based on EKF and elman neural network. In Proceedings of 2009 ICAL, Shenyang, China.
88. Bolognani S, Tubiana L, Zigliotto M (2003) Extended kalman filter tuning in sensorless PMSM drives. IEEE Trans Ind Appl 39(6):1741–1747
89. Mwasilu F, Jung JW (2016) Enhanced fault-tolerant control of interior PMSMs based on an adaptive EKF for EV traction applications. IEEE Trans Power Electron 31(8):5746–5758
90. Dhaouadi R, Mohan N, Norum L (1991) Design and implementation of an extended kalman filter for the state estimation of a permanent magnet synchronous motor. IEEE Trans Power Electron 6(3):491–497
91. Dang DQ, Rafaq MS, Choi HH, Jung J-W (2016) Online parameter estimation technique for adaptive control applications of interior PM synchronous motor drives. IEEE Trans Ind Electron 63(3):1438–1449
92. Rafaq MS, Mwasilu F, Kim J, Ho Choi H, Jung J-W (2017) Online parameter identification for model-based sensorless control of interior permanent magnet synchronous machine. IEEE Trans Power Electron 32(6):4631–4643
93. Kulkarni AB, Ehsani M (1992) A novel position sensor elimination technique for the interior permanent-magnet synchronous motor drive. IEEE Trans Ind Appl 28(1):144–150
94. Lee SB (2006) Closed-loop estimation of permanent magnet synchronous motor parameters by PI controller gain tuning. IEEE Trans Energy Convers 21(4):863–870
95. Ogasawara S, Akagi H (1998) An approach to real-time position estimation at zero and low speed for a PM motor based on saliency. IEEE Trans Ind Appl 34(1):163–168
96. Ogasawara S, Akagi H (1998) Implementation and position control performance of a IPM motor drive system based on magnetic saliency. IEEE Trans Ind Appl 34(4):806–812
97. Kim S-I, Im J-H, Song E-Y, Kim R-Y (2016) A new rotor position estimation method of IPMSM using all-pass filter on high-frequency rotating voltage signal injection. IEEE Trans Ind Electron 63(10):6499–6509

Han Woong Ahn received the B.S., M.S. and Ph.D. degrees in Electrical Engineering from Hanyang University, Seoul, Korea in 2010, 2012 and 2016, respectively. He is now working in Korea Aerospace Research Institute. His research interests include design, analysis, testing and control of motor/generator; power conversion systems; and applications of motor drive such as electric vehicles, high-speed maglev train and renewable energy systems.

Hyun Jong Park received his B.S., M.S. and PH.D. degrees in Electrical Engineering from Hanyang University, Seoul, Korea in 2009, 2011 and 2015, respectively. Since 2015, he is working in Korea Aerospace Research Institute. His research interests include design, analysis, testing and control of motor/generator; power conversion systems; applications of multi DOF motor for robots; and servo actuation system of gimballed engine and reaction control system for launch vehicle.

Chang Hyun Kim received his M.S and Ph.D in Electrical Engineering from Hanyang University, Korea, in 2006, and 2015, respectively. He was a senior researcher at Korea Marine Equipment Research Institute from 2015 to 2016. He is currently an assistant professor at VISION College of Jeonju, Korea. His current research interests include the robust control, MPC, optimal digital control, and its application to electric power grid, network congestion control, magnetic levitation systems, and so on.

Hyung-Woo Lee received his M.S. degree from Hanyang University, Seoul, Korea, in 2000, and his Ph.D. degree from Texas A&M University, College Station, TX, in 2003, both in Electrical Engineering. He was with Korea Railroad Research Institute as a Senior Reseacher from 2006 to 2013. He joined Korea National University of Transportation as an Professor of the department of Railway Vehicle System Engineering in March 2013. His research interests include design and analysis of motors/generators; and applications of motor drive, such as Maglev trains, conventional railway propulsion systems, and modern renewable energy systems.